Temperature Distribution in Workpiece During Flowdrill - Numerical Experiment Based on Meshless Methods

Anita Uscilowska(✉)

Faculty of Mechanical Engineering and Management,
Poznan University of Technology, Piotrowo 3, 60-965 Poznan, Poland
anita.uscilowska@put.poznan.pl

Abstract. The Flowdrill technology is quite new one. Is very promising technology, which could be applied in many industrial branches. This technology can be still developed. Moreover, to do modern research the numerical simulations are implemented for predicting the process duration, parameters of the process to obtain the product with demanded characteristics. The proposal of this paper is to implement one of so-called meshfree methods, i.e. Method of Fundamental Solutions, for computer simulation of temperature distribution in workpiece during Flowdrill process. In the basic approach The Method of Fundamental Solution is used for solving homogeneous boundary value problems. Due to the complexity of Flowdrill process proposed numerical algorithm for solving this problem is based on MFS supported by the Method Finite Differences and Picard Iterations. The paper consists of proposal of numerical algorithm based on MFS and results of numerical experiment. The main conclusion is that the MFS is sufficient method for simulations of processes of plastic deformations.

Keywords: Flowdrill · Temperature distribution ·
Method of Fundamental Solutions · Radial Basis Functions · Picard Iterations

1 Introduction

The Flowdrill technology is quite new one. The idea of thermal drilling was proposed by Jean Cloude de Valiere in 1923. But the useful tool started to be produced since 1980s. It's very promising technology, which could be applied in many industrial branches. The applications already made show many advantages of this technique and products obtained in this process. For example, Flowdrill technology is involved the automotive development process. The most important advantages of applying thermal drilling technology are cost reductions by using thinner material and shorter cycle time. The application in furniture industry is mostly based on low costs of connection of technical properties of joints obtained by Flowdrill and beautiful design of them. The other industry branches, which apply the Flowdrill technology are: loading equipment, railing construction, hospital equipment (for example wheel chairs), shopping charts, energy and sanitary systems (solar systems), cleaning systems, lighting, agriculture (plant and mast constructions), steel furniture, seatbelt construction and much more.

B. Gapiński et al. (Eds.): *Advances in Manufacturing II* - Volume 4, LNME, pp. 81–95, 2019.
https://doi.org/10.1007/978-3-030-16943-5_8

Generally saying, Flowdrill technology is a drilling method (making holes) which is capable of locally displacing material in order to form increased material thickness. The material is pushed out of the way with the aid of heat from friction. The temperature distribution is the crucial quantity of the process, because it influences on the properties of the material. The local heat production and heat flow makes material plastic. Thanks this fact the running of Flowdrill is possible. The process is also called friction drilling, thermal drilling, etc. The machine for thermal drilling is shown in Fig. 1 and tools for thermal drilling are presented in Fig. 2.

Fig. 1. Flowdrill machine.

Fig. 2. Thermoforming drill tool.

From technological point of view, the Flowdrill technology is used for making holes. The proposal of efficient use of boreholes by Flowdrill is presented in [1]. Authors of [1] checked the changing the properties of the material around the hole after application of the technology. The other purpose of using Flowdrill technology is thread connections (for example riveting, screw connection). The parameters of Flowdrill process of screwdriving were investigated by Authors of [2]. They proposed the quality design space as represented by resultant joint geometry as a function of the critical process parameters of fastener force and drilling speed. Identification of drilling parameters was the subject of the paper [3]. The experimental study has been performed to check influence of process parameters (rotational speed, drilling force, geometry of screw) on drilling time and torque. Very important aspect of screwdriving by Flowdrill is thermal effect. One of the papers related to this subject is [4]. Authors of this paper studied influence of different preprocess material temperatures on the

duration of the process. The preheating of material yields the shorter time of the process. The Flowdrill technology is used for sealing surface, as well. Is has applications for brazing and welding joints. It may be used as an alternative method for hole edge flanging. Authors of [5] considered characteristics of tools material dedicated for Flowdrill process. Their research includes study of microstructure and chemical composition (carbides phases), content of porosity in material of tool before and after drilling process.

Mostly, in literature it is stated that the Flowdrill is used for metal materials. But there are already some developments that point use of Flowdrill technology for other material than metals as well. For example, in [6] test for mechanical joints between fibre-reinforced plastics and metals was proposed. Both carbon-fibre-reinforced plastic and aluminium via a flow drill screw were connected. Moreover, in older literature, Flowdrill was indicated as a technology unusable for materials that have been painted, plastic coated, galvanized or heat treated. But, already one can find papers, as for example [7, 8] about materials with coating and galvanized, which were subjected to Flowdrill process. Authors investigated the influence of chemical structure of coating on the properties of the surface of drilled hole.

Moreover, to do modern research (save material - for workpiece and tools, energy, time) the numerical simulations are implemented for predicting the process duration, parameters of the process to obtain the product with demanded characteristics. Such calculations may be done by one of many numerical methods, which are known in literature. Most known and mostly applied is the Finite Element Method. For example, in papers [9–12] the computer simulations were presented for different types of joints. But this method has one disadvantage, which is very significant from plastic deformation point of view. The deformations are quite large, so the remeshing of FEM is strongly required. And it has to be done several times during process calculations. It makes the calculations very high time-consuming. The alternative methods are so-called meshfree methods. The implementation of one of such methods, i.e. Method of fundamental Solutions is proposed for temperature distribution simulation in Flowdrill process. The local heat production softenes the material and makes it plastic. So, it is important to know the temperature distribution, heat flow to estimate the heat affected zone, to predict plastic flow of the material.

Numerical simulations of temperature distribution during engineering processes is widely discussed in literature. Most interesting of the subject of the present paper are papers related to numerical simulations of technological processes made by meshless methods.

Authors of [13] have prepared the model of heat transfer during friction stir welding. In the paper, the thermal conductivity for work-piece and tool is taken to be constant. The problem is solved using meshless particle method. The obtained numerical results are in good agreement with those obtained from experiments.

The other work related to modeling of heat distribution during seam welding problems in [14]. Authors described the problem of heat transfer during the welding process by initial-boundary value problem. The computer simulation were done by Finite Difference Method (FDM). The numerical results were compared to results of the experiment. But Authors did not try to use meshless method instead of FDM, which does not require discretisation of a whole considered region.

The other technological processes were considered including heat transfer and solved by meshless methods in the literature, as well.

For example, the modelling and simulation of viscoplastic flow during an axisymmetric hot compression test of steel-like material were presented in [15]. The element-free Galerkin Method was implemented to perform numerical simulations of compression test. The results of calculations were used in an analysis of stress, strain state of the deformed probe.

One of the meshless methods was used by Authors of [16]. The subject of the paper is a determination of optimum cooling conditions for continuous casting. The considered problem has been solved by Improved Radial Point Interpolation Method. And Authors showed that this method is very suitable for solving non-linear transient problems.

The analytical and numerical solving the heat transfer problem is very widely discussed in the literature. One of the works related to meshless methods and solving heat transfer is [17]. In this work, Authors have used Direct Meshless Local Petrov-Galerkin method.

Authors of [18] presented the Trefftz Method applied for solving the inverse problem of heat transfer. The aim of their work was to calculate thermal conductivity coefficient of investigated materials. Meshless methods are very good tools to solve problems of an irregular domain (see [19]) and non-linear boundary conditions [20]. Authors of [21] presented solution of 1D and 2D transient problems of heat conduction. They proposed solving algorithm based on Trefftz Method using exponential basis functions. Also, composites as domains may be considered and issues with such domains are solved by meshless methods (see [22]).

A very large literature overview related to meshless methods applied for heat transfer and fluid flow problems is presented in [23].

2 Problem Description

The temperature distribution problem in workpiece during Flowdrill process may be modeled as an axisymmetric initial-boundary problem. The governing partially differential equation is of second order one with variable coefficients. The initial condition describes temperature of the whole workpiece at the beginning of Flowdrill process. The boundary condition describes temperature on the boundary of the workpiece at all time of process duration.

2.1 Mathematical Model

The geometry of the work piece is presented in Fig. 3.

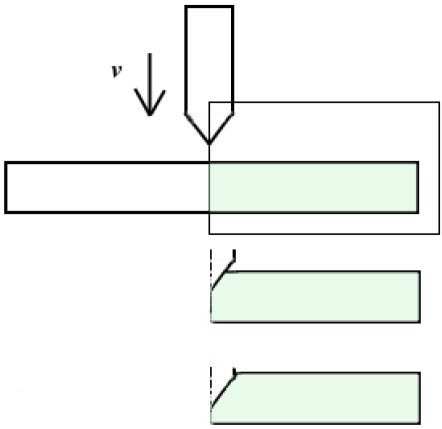

Fig. 3. Geometry of piecework.

Using the axisymmetry of the considered object the region of temperature distribution at initial time is presented in Fig. 4. and can be described as $\Omega = \{(x, y)|x_{\min} < x < x_{\max}, y_{\min} < y < y_{\max}\}$ with boundary $\Gamma = \Gamma_1 \cup \Gamma_2 \cup \Gamma_3 \cup \Gamma_4$, where

$$\Gamma_1 = \{(x, y)|x_{\min} < x < x_{\max}, y = y_{\min}\},$$
$$\Gamma_2 = \{(x, y)|x = x_{\max}, y_{\min} < y < y_{\max}\},$$
$$\Gamma_3 = \{(x, y)|x_{\min} < x < x_{\max}, y = y_{\max}\},$$
$$\Gamma_4 = \{(x, y)|x = x_{\min}, y_{\min} < y < y_{\max}\}.$$

The thickness of sheet is $h = y_{max} - y_{min}$.

The heat transfer equation is in the following form:

$$\rho c_p(T)\frac{\partial T}{\partial t} = \nabla \cdot (\lambda(T(x, y))\nabla T(x, y)) \text{ for } (x, y) \in \Omega \tag{1}$$

where t denotes time, T - temperature, x, y are geometrical coordinates, ρ is the density of the material, $c_p(T)$ - heat capacity of the material, $\lambda(T)$ - thermal conductivity coefficient.

The associated initial condition:

$$T(x, y, t_0) = T_0(x, y) \text{ for } (x, y) \in \Omega, \tag{2}$$

describes temperature in whole region Ω at initial time $t_0 = 0$.

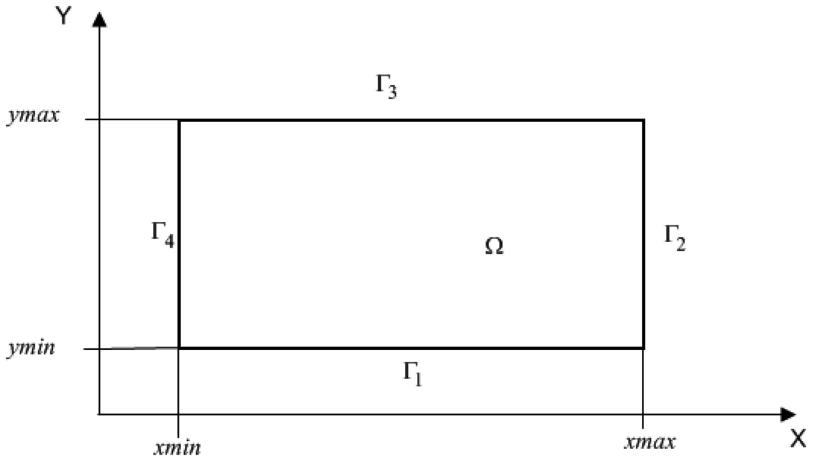

Fig. 4. Geometry of region Ω with boundary Γ at initial time.

It is assumed that on the boundary condition is described by function $g(x, y, t)$, so

$$B\,T(x, y, t) = g(x, y, t) \text{ for } (x, y) \in \Gamma \tag{3}$$

where operator B describes type of boundary condition. For boundary with defined temperature $B = 1$, for boundary with convection B is normal derivative of temperature. On the boundary, which has contact with the tool temperature is related to friction between the workpiece and the tool.

It is not so easy to set a particular value for material characteristics related to heat transfer. Therefore, the thermal conductivity coefficient $\lambda(T)$ and the heat capacity $c_p(T)$ will be treated as linear functions of temperature as follows:

$$\lambda(T) = \lambda_1 T + \lambda_0 \tag{4}$$

$$c_p(T) = c_{p1} T + c_{p0} \tag{5}$$

where $\lambda_1, \lambda_0, c_{p1}, c_{p0}$ are real numbers coefficients dependent on the material used for workpiece.

2.2 Numerical Algorithm

In case of Inhomogeneous Initial-Boundary Value Problem the Method of Fundamental Solutions cannot be introduced in pure form. It has to be supported by other methods.

The considered Eq. (1) consists of derivative of temperature concerning the time variable.

So, the problem will be solved in a certain interval of time. Let's notice that $t \in (0, t_{\max})$, where t denotes time variable, $t_{\max}$ is maximum value of the time variable.

First of all, to approximate time derivative, the method of finite differences is used. Time interval is divided into n_t subintervals. So, the solution will be calculated in certain time, i.e.

$$t_i = i \cdot dt, \text{ where } dt = \frac{t_{\max}}{n_t}.$$

So, the partial derivative at time equal to t_i is approximated by backward finite difference as follows

$$\left.\frac{\partial T(x,y,t)}{\partial t}\right|_{t=t_i} \approx \frac{T_i(x,y) - T_{i-1}(x,y)}{dt} \text{ for } i = 1, 2, \ldots, n_t \tag{6}$$

where $T_i(x,y) = T(x,y,t_i)$ denotes temperature at time t_i, i.e.

After using an approximation of partial derivative of temperature concerning the time, the initial-boundary value is changed into series of boundary value problems. For each time step the BVP is defined by equation

$$\begin{aligned} &\frac{\rho c_p(T_i(x,y))}{dt} T_i(x,y) - \nabla \cdot \left(\lambda(T_i(x,y)) \nabla T(x,y)|_{t=t_i}\right) \\ &= \frac{\rho c_p(T_{i-1}(x,y))}{dt} T_{i-1}(x,y) \end{aligned} \tag{7}$$

for $(x,y) \in \Omega$ and $i = 1, 2, \ldots, n_t$
and boundary conditions

$$T_i(x,y) = g(x,y,t_i) \text{ for } (x,y) \in \Gamma_3 \text{ and } i = 1, 2, \ldots, n_t, \tag{8}$$

$$\frac{\partial T_i(x,y)}{\partial n} = 0 \text{ for } (x,y) \in \Gamma_1 \cup \Gamma_2 \cup \Gamma_4 \text{ and } i = 1, 2, \ldots, n_t. \tag{9}$$

In Eq. (7) written for i = 1 the initial condition (2) is applied as $T(x,y,t_0) = T_0$.

The proposal of this paper is to implement the Method of Fundamental Solutions (MFS) to solve BVP given by Eqs. (7–9). MFS is a so-called analytical-numerical method. It is necessary to know analytical form of special function called "fundamental solution", which is determined for differential operator, which appears in the governing equation.

The Eq. (7) may be rewritten in the form

$$\begin{aligned} &\frac{\rho c_p(T_i(x,y))}{dt} T_i(x,y) - \frac{\partial \lambda(T_i(x,y))}{\partial T_i} \left(\left(\frac{\partial T_i(x,y)}{\partial x}\right)^2 + \left(\frac{\partial T_i(x,y)}{\partial y}\right)^2 \right) \\ &- \lambda(T_i(x,y)) \left(\frac{\partial^2 T_i(x,y)}{\partial x^2} + \frac{\partial^2 T_i(x,y)}{\partial y^2} \right) = \frac{\rho c_p(T_{i-1}(x,y))}{dt} T_{i-1}(x,y) \end{aligned} \tag{10}$$

for $(x,y) \in \Omega$ and $i = 1, 2, \ldots, n_t$

and we can notice that the differential operator consists of Laplace operator and square of first partial derivatives of temperature with respect to both geometrical variables. We will use the function "fundamental solution" for Laplace equation, therefore the Eq. (10) is rewritten in iterative mode (Picard iterations):

$$\frac{\partial^2 T_i^{(j)}(x,y)}{\partial x^2} + \frac{\partial^2 T_i^{(j)}(x,y)}{\partial y^2} = \left(\frac{\rho}{dt}\left(c_p\left(T_i^{(j-1)}(x,y)\right)T_i^{(j-1)}(x,y) - c_p(T_{i-1}(x,y))T_{i-1}(x,y)\right) - \frac{\partial\lambda\left(T_i^{(j-1)}(x,y)\right)}{\partial T_i^{(j-1)}}\left(\left(\frac{\partial T_i^{(j-1)}(x,y)}{\partial x}\right)^2 + \left(\frac{\partial T_i^{(j-1)}(x,y)}{\partial y}\right)^2\right)\right) \Big/ \lambda\left(T_i^{(j-1)}(x,y)\right) \tag{11}$$

for $(x,y) \in \Omega$ and $j = 1,2,\ldots n_j,\ i = 1,2,\ldots,n_t$
and the boundary conditions are

$$T_i^{(j)}(x,y) = g(x,y,t_i) \text{ for } (x,y) \in \Gamma_3 \text{ and } i = 1,2,\ldots,n_t,\ j = 1,2,\ldots n_j \tag{12}$$

$$\frac{\partial T_i^{(j)}(x,y)}{\partial n} = 0 \text{ for } (x,y) \in \Gamma_1 \cup \Gamma_2 \cup \Gamma_4 \text{ and } i = 1,2,\ldots,n_t,\ j = 1,2,\ldots n_j \tag{13}$$

where n_j is the number of iteration made at each time step and $T_i^{(j)}(x,y)$ denotes temperature at j-th iteration of i-th time step.

So, at each iteration at every time step there is BVP to be solved. To simplify notation for describing the next step of iterations, the BVP (11–13) is written in form:

– equation

$$\frac{\partial^2 T_i^{(j)}(x,y)}{\partial x^2} + \frac{\partial^2 T_i^{(j)}(x,y)}{\partial y^2} = f\left(x,y,T_i^{(j-1)}(x,y), T_{i-1}(x,y)\right) \tag{14}$$

for $(x,y) \in \Omega$ and $j = 1,2,\ldots n_j,\ i = 1,2,\ldots,n_t$
where

$$f\left(x,y,T_i^{(j-1)}(x,y), T_{i-1}(x,y)\right) = \left(\frac{\rho c_p\left(T_i^{(j-1)}(x,y)\right)}{dt}\left(T_i^{(j-1)}(x,y) - T_{i-1}(x,y)\right) - \frac{\partial\lambda\left(T_i^{(j-1)}(x,y)\right)}{\partial T_i^{(j-1)}}\left(\left(\frac{\partial T_i^{(j-1)}(x,y)}{\partial x}\right)^2 + \left(\frac{\partial T_i^{(j-1)}(x,y)}{\partial y}\right)^2\right)\right) \Big/ \lambda\left(T_i^{(j-1)}(x,y)\right) \tag{15}$$

– boundary conditions

$$BT_i^{(j)}(x,y) = g(x,y,t_i) \text{ for } (x,y) \in \Gamma \text{ and for } j = 1,2,\ldots n_j \text{ and } i = 1,2,\ldots,n_t, \quad (16)$$

where $B = 1$.

The MFS is the numerical method for solving BVP described by homogeneous partially differential equation. The Eq. (14) is inhomogeneous one, therefore the MFS is supported by approximation by Radial Basis Functions (RBFs) and monomials. Such approach of solving is known in literature as Dual Reciprocity Method. The solution of inhomogeneous BVP is assumed to be sum of particular and homogeneous solution:

$$T_i^{(j)}(x,y) = T_{p,i}^{(j)} + T_{h,i}^{(j)} \quad (17)$$

where $T_{p,i}^{(j)}$, $T_{h,i}^{(j)}$ are, respectively, particular and homogeneous solution of Eq. (14).

The particular solution is found by approximation of right-hand side function $f\left(x,y,T_i^{(j-1)}(x,y),T_{i-1}(x,y)\right)$ by RBFs and monomials as:

$$f\left(x,y,T_i^{(j-1)}(x,y),T_{i-1}(x,y)\right) = \sum_{k=1}^{na} a_k \varphi\left(r_k^{(a)}(x,y)\right) + \sum_{k=1}^{nm} a_{na+k}\, p_k(x,y) \quad (18)$$

where $\varphi\left(r_k^{(a)}(x,y)\right)$ (for $k = 1,\ldots,n_a$) are RBFs, $p_k(x,y)$ (for $k = 1,\ldots,n_m$) are monomials, a_k (for $k = 1,\ldots,n_a + n_m$) are real numbers, n_a – number of approximation points, n_m – number of monomials. The set of approximation points $\left\{x_k^{(a)}, y_k^{(a)}\right\}$ (for $k = 1,\ldots,n_a$) is defined and quantity $r_k^{(a)}(x,y)$ is defined as: $r_k^{(a)}(x,y) = \sqrt{\left(x - x_k^{(a)}\right)^2 + \left(y - y_k^{(a)}\right)^2}$. The approximation is done for every approximation point, which gives the system of linear algebraic equations

$$\begin{aligned} &\sum_{k=1}^{na} a_k \varphi\left(r_k^{(a)}\left(x_l^{(a)}, y_l^{(a)}\right)\right) + \sum_{k=1}^{nm} a_{na+k} p_k\left(x_l^{(a)}, y_l^{(a)}\right) \\ &= f\left(x_l^{(a)}, y_l^{(a)}, T_i^{(j-1)}\left(x_l^{(a)}, y_l^{(a)}\right), T_{i-1}\left(x_l^{(a)}, y_l^{(a)}\right)\right) \end{aligned} \quad (19)$$

for $l = 1,\ldots,n_a$.

Once, the parameters a_k (for $k = 1,\ldots,n_a + n_m$) are calculated, the particular solution is:

$$T_{p,i}^{(j)}(x,y) = \sum_{k=1}^{na} a_k \psi\left(r_k^{(a)}(x,y)\right) + \sum_{k=1}^{nm} a_{na+k} P_k(x,y) \quad (20)$$

where $\psi(r)$ and $P_k(x,y)$ for $k = 1,\ldots,n_m$ are particular solutions of Poisson equation with inhomogeneous part of $\varphi(r)$ and $p_k(x,y)$ for $k = 1,\ldots,n_m$, respectively.

In this paper the Radial Basis Functions $\varphi(r) = r^2 \ln r$ and monomials $p_1(x,y) = 1$, $p_2(x,y) = x$, $p_3(x,y) = x^2$, $p_4(x,y) = y$, $p_5(x,y) = y^2$, $p_6(x,y) = xy$ are used. The particular solutions for these functions are $\psi(r) = 0.25r^4(\ln r - 0.5)$, $P_1(x,y) = (x^2+y^2)/4$, $P_2(x,y) = (x^2+y^2)x/6$, $P_3(x,y) = (x^4 + x^2y^2 - y^4/6)/14$, $P_4(x,y) = (x^2+y^2)\,y/6$, $P_5(x,y) = (-x^4/6 + x^2y^2 + y^4)/14$, $P_6(x,y) = xy(x^2+y^2)/12$.

Next step of numerical procedure is to calculate homogeneous solution. It is done by using the boundary conditions as

$$BT_{h,i}^{(j)}(x,y) = g(x,y,t_i) - BT_{p,i}^{(j)}(x,y) \tag{21}$$

In MFS it is assumed that the homogeneous solution is a linear combination of functions "fundamental solution":

$$T_{h,i}^{(j)}(x,y) = \sum_{k=1}^{ns} c_k fs\left(r_k^{(s)}(x,y)\right) \tag{22}$$

where $fs(r)$ is the fundamental solution function, $r_k^{(s)}(x,y) = \sqrt{\left(x - x_k^{(s)}\right)^2 + \left(y - y_k^{(s)}\right)^2}$, $\left\{x_k^{(s)}, y_k^{(s)}\right\}$ for $k = 1,\ldots,n_s$, is a set of source points, which are placed outside the region Ω, n_s is a number of source points, s is a distance between boundary Γ and fictitious boundary with source points, c_k $(k = 1,\ldots,n_s)$ – real number coefficients.

To obtain the numbers c_k $(k = 1,\ldots,n_s)$ the boundary Γ is discretised, i.e. the set $\left\{x_k^{(b)}, y_k^{(b)}\right\}$ for $k = 1,\ldots,n_b$, of boundary points $\left(x_k^{(b)}, y_k^{(b)}\right) \in \Gamma$ is chosen. Number n_b is a number of boundary points. Then, the boundary condition (22) is written for each boundary point, so

$$\sum_{k=1}^{ns} c_k Bfs\left(r_k^{(s)}(x,y)\right)\Big|_{\substack{x = x_l^{(b)} \\ y = y_l^{(b)}}} = g\left(x_l^{(b)}, y_l^{(b)}, t_i\right) - BT_{p,i}^{(j)}\left(x_l^{(b)}, y_l^{(b)}\right) \tag{23}$$

for $l = 1,\ldots,n_s$.

The fundamental solution for Laplace equation is $fs(r) = \ln r$. The solutions of given above system of linear algebraic Eq. (23) are numbers c_k $(k = 1,\ldots,n_s)$. So, the final solution for j-th iteration at i-th time step is obtained.

The procedure of calculation of j-th iterations at i-th time step is stopped when the following condition

$$\frac{1}{n_t}\sum_{k=1}^{nt}\left|T_i^{(j)}\left(x_k^{(t)}, y_k^{(t)}\right) - T_i^{(j-1)}\left(x_k^{(t)}, y_k^{(t)}\right)\right| < \varepsilon \tag{24}$$

where $\left\{x_k^{(t)}, y_k^{(t)}\right\}$ is a set of trial points placed in region Ω, n_t is a number of trial points, ε - small number, is fulfilled.

3 Numerical Results

The numerical experiment has been preformed to validate the proposed algorithm.

The parameters of the MFS were chosen by checking some conditions, which are described below.

The parameters s, n_b, n_s are chosen by checking the fulfilling of boundary conditions. If the inequality

$$\frac{1}{n_{tb}}\sum_{k=1}^{ntb}\left|g\left(x_k^{(tb)},y_k^{(tb)},t_i\right)-T_i^{(j)}\left(x_k^{(tb)},y_k^{(tb)}\right)\right|<\varepsilon \tag{25}$$

is the truth the values of s, n_b, n_s are treated as an optimal choice. In formula (25) $\left\{x_k^{(tb)},y_k^{(tb)}\right\}$ for $k=1,\ldots,n_{tb}$, is a set of trial points placed on boundary Γ and n_{tb} is a number of chosen boundary trial points.

The number of boundary points is chosen as 40. The boundary points are uniformly distributed on boundary (10 points for each edge of rectangular domain). Number of source points is 40, distance $s = 0.2$. Source points were placed on the boundary of rectangular similar to the domain Ω with length of edges $(x_{\max}-x_{\min}+2s)$ and $(y_{\max}-y_{\min}+2s)$.

Number of approximation points n_a is chosen for each time step by checking the following condition:

$$\begin{aligned}&\frac{1}{n_t}\sum_{k=1}^{nt}\left|f\left(x_k^{(t)},y_k^{(t)},T_i^{(j-1)},T_{i-1}\right)\right.\\&\left.-\sum_{k=1}^{na}a_k\varphi\left(r_k^{(a)}\left(x_k^{(t)},y_k^{(t)}\right)\right)-\sum_{k=1}^{nm}a_{na+k}p_k\left(x_k^{(t)},y_k^{(t)}\right)\right|<\varepsilon\end{aligned} \tag{26}$$

The number of approximation points was calculated as 121 and they are placed in the domain Ω.

So, the calculations were made using the iteration stop condition (26) with the value of accuracy parameter ε equal to 10^{-5}. Number of iterations steps required at each time step to obtain the solution with demanded accuracy is given in Table 1.

Table 1. Number of iterations steps.

Time step	1	2	3	4	5	6	7	8
Number of iterations	4	5	5	5	6	5	5	5

We can observe that the proposed procedure is rather low time and work consuming. Just 4–6 iterations at each time steps are done to obtain results with demanded accuracy.

To estimate the fulfilling of the boundary conditions and correctness of done approximation of non-homogeneous part of the differential equation the values of following quantities

$$\varepsilon_b = \frac{1}{n_{tb}} \sum_{k=1}^{ntb} \left| g\left(x_k^{(tb)}, y_k^{(tb)}, t_i\right) - BT_i^{(j)}\left(x_k^{(tb)}, y_k^{(tb)}\right) \right| \tag{27}$$

$$\varepsilon_a = \frac{1}{n_t} \sum_{k=1}^{nt} \left| f\left(x_k^{(t)}, y_k^{(t)}, T_i^{(j-1)}, T_{i-1}\right) - \sum_{k=1}^{na} a_k \varphi\left(r_k^{(a)}\left(x_k^{(t)}, y_k^{(t)}\right)\right) - \sum_{k=1}^{nm} a_{na+k} p_k\left(x_k^{(t)}, y_k^{(t)}\right) \right| \tag{28}$$

has been calculated and presented in Table 2. We can notice that ε_a and ε_b are rather small numbers and confirm the good choice of values of parameters s, n_b, n_s.

Table 2. Values of ε_b, ε_a.

i-th time step	j-th iteration	ε_a	ε_b
1	1	2 · 10e−6	1 · 10e−6
	2	2 · 10e−6	3 · 10e−6
	3	3 · 10e−6	4 · 10e−6
	4	3 · 10e−6	6 · 10e−6
2	1	8 · 10e−6	3 · 10e−6
	2	7 · 10e−6	3 · 10e−6
	3	4 · 10e−6	4 · 10e−6
	4	4 · 10e−6	4 · 10e−6
	5	5 · 10e−6	5 · 10e−6

The distribution of temperature is plotted in graphs presented in Fig. 5. One can observe the change of the region shape at the following time steps. It is due to movement of the tool. The region of the heat affected zone is can be noticed. The maximum temperature is at the boundary which is in contact with the tool. And it is easy to observe the convection condition of the upper surface of the workpiece. The vertical surface of the workpiece has temperature equal to ambient temperature. It means that the heat affect zone does not occupy the whole region.

We can conclude that in that region of increased temperature the material becomes more soft and plastic, and material will perform plastic flow in this region.

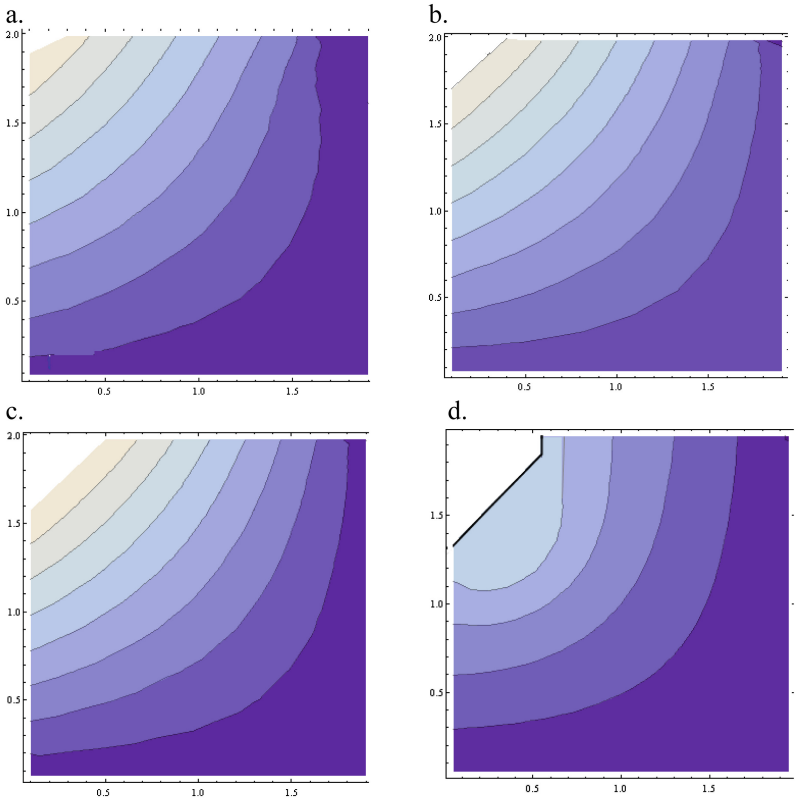

Fig. 5. Temperature distribution in region in following time step: a. 0.2 s, b. 0.4 s, c. 0.5 s, d. 0.6 s.

4 Conclusions

The technology of Flowdrill, as a quite new one, requires still wild research. One of branches of investigation may be numerical experiment. In this paper the innovative proposal and implementation of one of meshless method was presented. The Method of Fundamental Solution was a base of proposed numerical algorithm, supported by Method of Finite Differences, approximation by Radial Basis Functions and Picard Iterations.

Presented complex method was tested, with validation of the method parameters. When the accuracy of the method was checked the problem of temperature distribution in the workpiece under Flowdrill process was simulated. The results of this numerical experiment are consistent with expectations. So, we may conclude that the proposed combination of some chosen numerical methods, based on MFS is a good tool to simulate phenomenum of temperature distribution during Flowdrill process.

References

1. Mascenik, A., Pavlenko, S.: Effective use of technology Flowdrill in production engineering. Adv. Mater. Res. **1064**, 171–174 (2015)
2. Skovron, J., Mears, L., Ulutan, D., Detwiler, D., Paolini, D., Baeumler, B., Claus, L.: Characterization of flow drill screwdriving process parameters on joint quality. SEA Int. J. Mater. Manuf. **8**(1), 35–44 (2015)
3. Aslan, F., Langlois, L., Mangin, P., Balan, T.: Identification of drilling parameters during the flow drill screw driving process. Key Eng. Mater. **767**, 465–471 (2018)
4. Skovron, J., Prasad, R.R., Ulutan, D., Mears, L., Detwiler, D., Paolini, D., Baeumler, B., Claus, L.: Effect of thermal assistance on the joint quality of Al6063-T5A during flow drill screwdriving. J. Manuf. Sci. Eng. **137**(5), 51019–51027 (2015)
5. Matysiak, W., Bartkowski, D., Frackowiak, P.: Microstructure, mocrohardness and general characterisation of sintered tools using for flanging of hole edge by Flowdrill technology. In: IOP Conference Series: Materials Science and Engineering, vol. 393, p. 012094 (2018)
6. Szlosarek, R., Karalt, T., Enzinger, N., Hahne, C., Meyer, N.: Mechanical testing of flow drill screw joints between fibre-reinforced plastics and metals. Materails Test **55**(10), 737–742 (2013)
7. Bartkowski, D., Matysiak, W., Bartkowska, A.: Selected properties of laser cladding coatings shaped using flow drill technology. In: MATEC Web of Conferences, vol. 137, p. 05001 (2017)
8. Matysiak, W., Bartkowski, D., Bartkowska, A.: Selected properties of galvanic coatings shaped using thermal drilling technology. In: MATEC Web of Conferences, vol. 137, p. 05004 (2017)
9. Yamashita, M., Kenmotsu, H., Hattori, T.: Dynamic crush behavior of adhesive-bonded aluminum tubular structure - experiment and numerical simulation. Thin-Walled Struct. **69**, 45–53 (2013)
10. Hanssen, A.G., Olovsson, L., Porcaro, R., Langseth, M.: A large-scale finite element point-connector model for self-piercing rivet connections. Eur. J. Mech. A/Solids **29**, 484–495 (2010)
11. Carlberger, T., Stigh, U.: Dynamics testing and simulation of hybrid joined bi-material beam. Thin-Walled Struct. **48**, 609–619 (2010)
12. KolstøSønstabø, J., Morin, D., Langseth, M.: Macroscopic modelling of flow-drill Screw connections in thin-walled aluminium structures. Thin-Walled Struct. **105**, 185–2016 (2016)
13. Xiao, Y., Zhan, H., Gu, Y., Li, Q.: Modeling heat transfer during friction stir welding using a meshless particle method. Int. J. Heat Mass Transf. **104**, 288–300 (2017)
14. Huang, J.-H., Ngo, T.-T., Wang, C.-C.: HSDM and BFGS method for determining the heat generation and range of heat distribution in 2-D ultrasonic welding problems. Numer. Heat Transf. Part B: Fundam. **69**(1), 48–67 (2016)
15. Alvarez, J.C., Bencomo, A.D., Cabrera, E.S.P., Guerin, J.-D., Dubar, L.: Modeling the viscoplastic flow behavior of a 20MnCr5 steel grade deformed under hot-working conditions, employing a meshless technique. Int. J. Plast **103**, 119–142 (2018)
16. Khosravifard, A., Hematiyan, M.R., Marin, L.: Determination of optimum cooling conditions for continuous casting by a meshless method. J. Mech. Eng. Sci. **227**(5), 1022–1035 (2012)
17. Mirzaei, D., Schaback, R.: Solving heat conduction problems by the direct meshless local Petrov-Galerkin (DMLPG) method. Numer. Algorithms **65**(2), 275–291 (2014)
18. Maciag, A., Walaszczyk, M.: The usage of the Trefftz method to determine the Biot number. J. Appl. Math. Comput. Mech. **16**(4), 47–55 (2017)

19. Fan, H., Zhang, D., Yu, H.: Collocation Trefftz method for the heat conduction issue in irregular domain. Adv. Mater. Res. **516–517**, 146–155 (2012)
20. Fan, H., Yu, H., Zhang, D.: Collocation Trefftz method for the heat conduction issue in irregular domain with non-linear boundary condition. Adv. Mater. Res. **516–517**, 156–164 (2012)
21. Movahedian, B., Boroomand, B., Soghrati, S.: A Trefftz method in space and time using exponential basis functions: application to direct and inverse hest conduction problems. Eng. Anal. Boundary Elem. **37**, 868–883 (2013)
22. Zmindak, M., Pelagis, A., Dudinsky, A.: MFS heat conduction modelling of composite materials reinforced by CNT-fibers with large aspect ratio. Appl. Mech. Mater. **420**, 202–208 (2013)
23. Rajul, G., Thakur, H.Ch., Brajesh, T.: A review of applications of meshfree methods in the area of heat transfer and fluid flow: MLPG method in particular. Int. Res. J. Eng. Technol. **2**(4), 329–338 (2015)